Available online at www.sciencedirect.com
SCIENCE DIRECT
Tetrahedron 62 (2006) 8591–8600
Tetrahedron

Tröger's base scaffold in racemic and chiral fashion as a spacer for bisdistamycin formation. Synthesis and DNA binding study

Martin Valík,[a] Jaroslav Malina,[b] Lukáš Palivec,[a] Jarmila Foltýnová,[a] Marcela Tkadlecová,[a] Marie Urbanová,[c] Viktor Brabec[b] and Vladimír Král[a,*]

[a]*Institute of Chemical Technology Prague, Dept. of Analytical Chemistry, Technická 5, 166 28 Prague 6, Czech Republic*
[b]*Institute of Biophysics, Academy of Sciences of the Czech Republic, Královopolská 135, 612 65 Brno, Czech Republic*
[c]*Institute of Chemical Technology Prague, Dept. of Physics and Measurements, Technická 5, 166 28 Prague 6, Czech Republic*

Received 21 February 2006; revised 29 May 2006; accepted 15 June 2006
Available online 14 July 2006

Abstract—'Head-to-head' oligo-*N*-methylpyrrole peptide dimers linked by a methano[1,5]diazocin scaffold are presented in racemic as well as chiral fashion. Their DNA binding activities were assayed on calf thymus DNA, poly(dA-dT)$_2$, and poly(dC-dG)$_2$ by NMR and ECD spectroscopies, and fluorescence probe displacement assay. The presented dimers prefer AT sequences, but show higher affinity to poly(dC-dG)$_2$ than distamycin A. The (4*R*,9*R*) configuration of methanodiazocin bridge was found to be better suited for interaction with ct-DNA and poly(dA-dT)$_2$ than (4*S*,9*S*) configuration.
© 2006 Elsevier Ltd. All rights reserved.

1. Introduction

The low molecular weight, sequence selective agents that interact with double-stranded DNA have been studied over four decades.[1] These molecules are mainly based on natural products, which bind to the minor groove of DNA. One of the most studied minor groove binders is distamycin A (Fig. 1, **1**)[2] and its analogues.[1,3–5]

Distamycin A is naturally occurring antibiotic agent that can reversibly bind to the minor groove of DNA by hydrogen and van der Waals bonds, and electrostatic interactions. Solution NMR spectroscopy[6,7] and X-ray diffraction[8] studies established a strong preference of distamycin A for adenine–thymine (AT) rich sequences containing at least four AT base pairs. In addition, extension of the number of pyrrole units in distamycin A analogues increased the sequence specificity for longer tracts of AT rich DNA,[9,10] and replacing *N*-methylpyrrole (Py) by *N*-methylimidazole (Im) ring changed the selectivity from AT to the cytosine–guanosine (CG) base pair.[11,12] NMR[13,14] and footprinting[15,16] experiments showed that distamycin A and its homologues can bind DNA as monomers as well as antiparallel dimers.

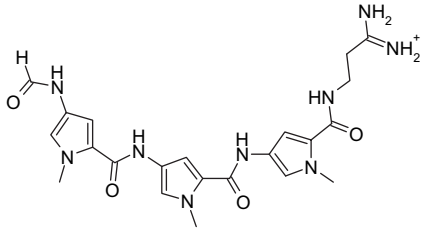

1

Figure 1.

Based on this understanding, covalently linked oligopeptide dimers have been prepared, which were coupled in antiparallel 'head-to-tail' fashion with various linkers.[4,5,17–19] These covalent linkages of two oligopeptides form the ligands with a U-shape motif, which binds to DNA with both increased affinity and specificity, as compared to the unlinked oligopeptides. For instance, dimer ImPyPy-PyPyPy linked by γ-aminobutyric acid binds to 5′-TGTTA-3′ with more than 2 orders of magnitude greater affinity than the unlinked oligopeptides, ImPyPy and PyPyPy.[17]

The parallel 'tail-to-tail'[20] and 'head-to-head'[21–30] linked oligopeptide dimers have been designed as bidentate DNA binders. In the case of 'head-to-head' dimeric oligopeptides, it was found that conformationally constrained cycloalkane and *trans*-alkenic linkers[28] prove higher effectivity for their bidentate binding to DNA than flexible polymethylene linked chains.[26,27] In addition, the stereochemistry of the linkers is also important and can control the binding.[23,29] To the best of our knowledge, only two examples of DNA binding studies of 'head-to-head' dimeric oligopeptides

Keywords: Tröger's base; Distamycin dimer; Enantioselective binding; Dissymmetry factor; VCD.
* Corresponding author. E-mail: kralv@vscht.cz

0040–4020/$ - see front matter © 2006 Elsevier Ltd. All rights reserved.
doi:10.1016/j.tet.2006.06.056

with an optically active linker have been reported to date.[23,29] And the problem of ideal shape and stereochemistry of linker for bidentate binding is still unclear.

In order to obtain structural information and further insights into chiral discrimination in the binding of optically active 'head-to-head' dimeric oligopeptides to DNA, we report in this study a constrained system of dimeric oligo-*N*-methylpyrrole peptides linked by the methano[1,5]diazocin scaffold, which fashions Tröger's base (TB) derivatives. The unique V-shape geometry (81–104°) of TB and the inherent chirality have been used in the construction of various receptors.[31–33] Moreover, some heterocyclic TB derivatives including phenanthroline and acridine interact specifically and enantioselectively with DNA.[34–36] The design of presented oligo-*N*-methylpyrrole peptide dimers also involved the width of linkers, which was established to be approximately 8 Å. The size of linkers should not cause steric restraints on binding of proposed dimers to the minor groove of DNA that is 10 Å wide.[37] In addition, the groove width in DNA–distamycin complexes was determined from 7 to 14 Å.[13,37,38] We rationalized that the interconnection of two distamycin analogues with methanodiazocin scaffold of TB could afford enantio-selective bidentate minor groove binders.

2. Results and discussion

2.1. Synthesis

As we described previously,[39] direct preparation of such compounds by methanodiazocin bridging of the corresponding amino-monomers is unsuccessful because degradation effects predominate. The synthetic strategy is based on the extension of central 4,9-methano-1,6-dimethyl-4,5,9,10-tetrahydro-1*H*,6*H*-dipyrrolo-[3,2-*b*:3′,2′-*f*][1,5]diazocin-2,7-dicarboxylate core via amide coupling of active ester precursor **2** and amino-arm.

Active ester precursor **2** was obtained in four steps by reaction sequences shown in Scheme 1. Benzyl 1-methyl-4-nitropyrrole-2-carboxylate (**3**) was prepared as described elsewhere.[40] The following reduction[41,42] of nitro group was achieved by nickel boride (Ni_2B) to give amine hydrochloride[43] **4**. Treatment of **4** with aqueous solution of formaldehyde regioselectively gave TB analogue **5**.[39] Catalytic hydrogenation of benzyl ester groups of **5** yielded dicarboxylic derivative **6** that was subsequently converted to active ester **2** by its reaction with 1-hydroxy benzotriazole (HOBt) and *N*,*N*′-dicyclohexylcarbodiimide (DCC).

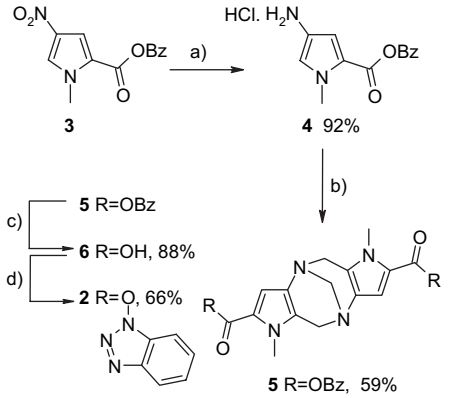

Scheme 1. Reagents and conditions: (a) Ni_2B, aqueous concd HCl, methanol, 70 °C; (b) aqueous concd H_2CO, aqueous concd HCl, ethanol, rt; (c) H_2, Pd/C, DMF, rt; (d) DCC, HOBt, DMF, CH_2Cl_2, rt.

The active ester **2** was then used for the preparation of methanodiazocin bridged dimeric oligo-*N*-methylpyrrole derivatives via amide protocol with amines[40] **7–10** (see Scheme 2). Products **11–14** were separated from reaction mixtures by column chromatography on silica with 5% concd aqueous ammonia in methanol as an eluent. The most effective DNA-binder **14** was then prepared in both optically pure forms (4*R*,9*R*)-**14** and (4*S*,9*S*)-**14** by a similar synthetic method.

Enantiomeric synthesis came from an analogue of benzyl ester **5**, 1-phenylethyl ester **15** that is easily obtainable in the optically pure state as we have recently described.[42] Conversion of 1-phenylethyl esters **15a** and **15b** (Fig. 2) into active esters (4*R*,9*R*)-**2** and (4*S*,9*S*)-**2** were performed without separation of acid **6** due to racemization hazard of methanodiazocin bridge. Note that acid (4*R*,9*R*)-**6** and (4*S*,9*S*)-**6** were also prepared due to better band assignment in IR

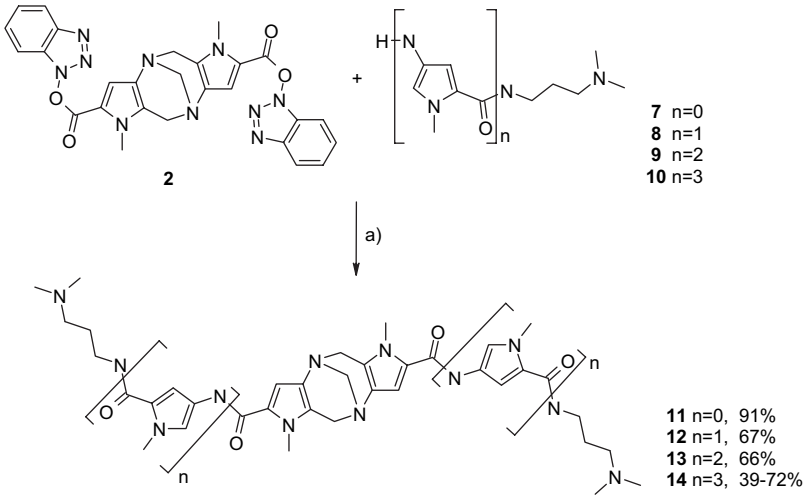

Scheme 2. Reagents and conditions: (a) DMF, amine, 60 °C.

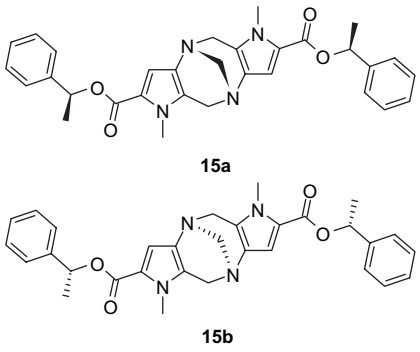

Figure 2.

and vibrational CD (VCD) spectra of (4*R*,9*R*)-**14** and (4*S*,9*S*)-**14**. The optical stability of active esters (4*R*,9*R*)-**2** and (4*S*,9*S*)-**2**, as well as dimers (4*R*,9*R*)-**14** and (4*S*,9*S*)-**14** was confirmed by ECD (see Fig. 3, ECD spectra of final dimer (4*R*,9*R*)-**14** and (4*S*,9*S*)-**14**) and optical rotation measurements of both enantiomers.

The structures of all prepared compounds were verified by detailed analyses of ^{1}H, ^{13}C, 1D NOESY, gHSQC, gHMBC, and gCOSY NMR experiments. The optically pure acids (4*R*,9*R*)-**6** and (4*S*,9*S*)-**6** and dimers (4*R*,9*R*)-**14** and (4*S*,9*S*)-**14** were then investigated by VCD that is a powerful tool for the description of chiral systems, like prediction of conformation of macromolecules,[44–47] determination of absolute configuration of molecules,[48] and interaction studies[49,50] of molecules as well as macromolecules.[51]

The racemate **14** and enantiomers (4*S*,9*S*)-**14** and (4*R*,9*R*)-**14** provide identical IR absorption spectra in the measured region 1800–1100 cm^{-1} (see Fig. 4B). The VCD spectra of (4*S*,9*S*)-**14** and (4*R*,9*R*)-**14** are nearly symmetrical (mirror-image) with respect to baseline. The baseline was obtained as VCD spectrum of racemate **14** and it was close to zero. The characteristic vibrations of pyrroles and amide I (1800–1350 cm^{-1}) are well separated from the characteristic vibrations of methanodiazocin bridge [52] (1350–1100 cm^{-1}).

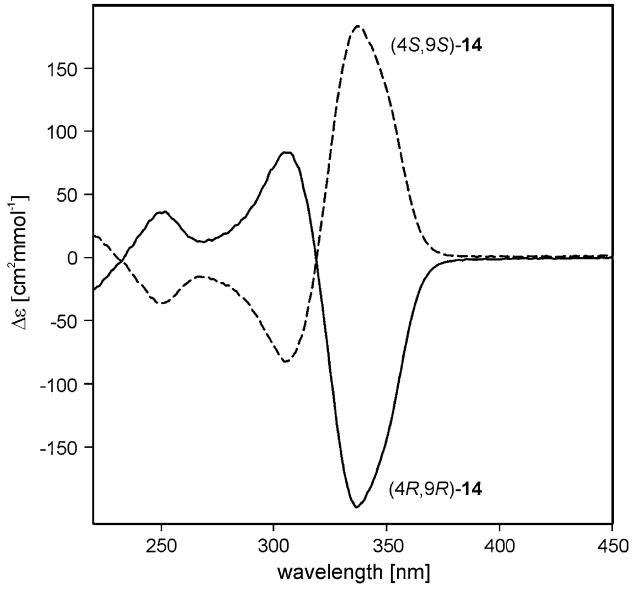

Figure 3. ECD spectra of final dimer (4*R*,9*R*)-**14** and (4*S*,9*S*)-**14**.

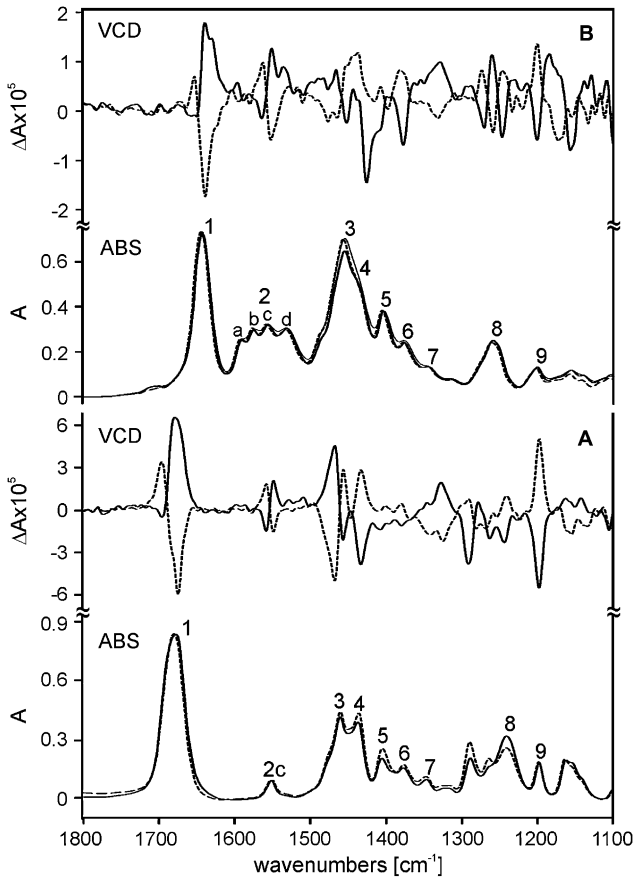

Figure 4. VCD and IR absorption spectra of (A) (4*S*,9*S*)-**6** (dashed line) and (4*R*,9*R*)-**6** (solid line), and (B) (4*S*,9*S*)-**14** (dashed line) and (4*R*,9*R*)-**14** (solid line), and IR absorption of **14** racemate (solid thin line) in $(CD_3)_2SO$.

However, we were not able to resolve the vibration of *N*-methylpyrroles that are bridged by methanodiazocin, and the vibrations of *N*-methylpyrroles from the tripeptidic arms. Moreover, the bands of the methanodiazocin bridge are overlapped by the bands of *N*-methylpyrroles and *N*,*N*-dimethylaminopropyl terminals (see Table 1 and Fig. 4B, Peak no. 4, 7, and 8).

Table 1. Characteristic IR vibrations of acid **6** and dimer **14** in $(CD_3)_2SO$, 1100–1800 cm^{-1} spectral region

Band No.	Wavenumbers [cm^{-1}]		Characteristic vibrations
	Acid **6**	Dimer **14**	
1	1680	1643	C=O stretch: –COOH group (for **6**), amide I (for **14**)
2a		1591	C=C stretch: pyrrole
2b		1575	C=C stretch: pyrrole
2c	1550	1557	C=C stretch: pyrrole of central core
2d		1531	C=C stretch: pyrrole
3	1461	1455	CH_3 asymmetric bend
4	1435	1432	CH_2 bend (scissor)
5	1404	1404	Ring vibration: pyrrole
6	1376	1376	CH_3 symmetric bend
7	1344	1344	CH_3 and CH_2 deformation
8	1241	1259	C–N stretch: methanodiazocin bridge, *N*-methylpyrrole groups+ *N*,*N*-dimethylamino group (for **14**)
9	1201	1201	C–N stretch: methanodiazocin bridge

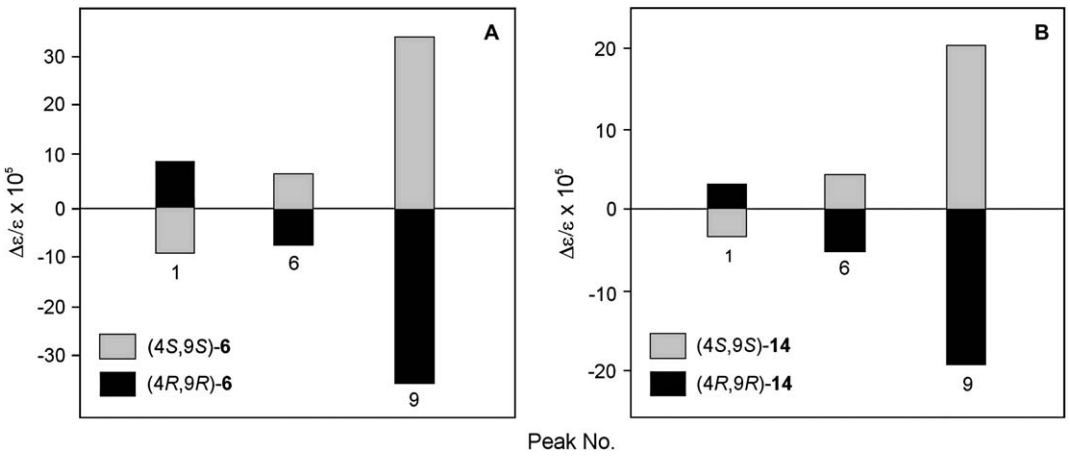

Figure 5. VCD dissymmetry factor $\Delta\varepsilon/\varepsilon$ of selected bands of (A) **6** and (B) **14**.

IR and VCD spectra of enantiomers of **6**, the compound representing the di-*N*-methylpyrrolomethanodiazocin core, were studied in parallel to elucidate the assignment of vibration bands of **14** (see Fig. 4 and Table 1). Enantiomers (4*S*,9*S*)-**6** and (4*R*,9*R*)-**6** also provide identical IR absorption spectra and mirror-image VCD spectra as observed for (4*S*,9*S*)-**14** and (4*R*,9*R*)-**14**.

The absorption band at 1557 cm^{-1} (2c) was assigned to *N*-methylpyrroles of the central core of **14** because this band is also present in spectra of **6** at 1550 cm^{-1} (2c) and the VCD pattern corresponding to these absorption bands are almost the same. The other bands (2a, 2b, and 2d) were assigned to *N*-methylpyrroles of the tripeptide arms of **14** and do not possess VCD signals. The bands at 1680 and 1643 cm^{-1} (1) were assigned to C═O vibration of carboxylic group of **6** and the amide group of **14**, respectively. The CH_3 bend vibrations (3, 6, and 7), the CH_2 bend vibrations (4 and 7), the ring vibration of pyrroles (5), and C–N vibrations (8 and 9) were observed in the absorption spectra of acid **6** as well as dimer **14**.

2.2. Asymmetry transfer evolution

Dissymmetry factor[53,54] (ratio of intensity of VCD signal and the intensity of corresponding IR signal, $\Delta\varepsilon/\varepsilon$) values calculated for characteristic vibrations were used to describe the distribution of asymmetry in both molecules **6** and **14**. Generally, $\Delta\varepsilon/\varepsilon$ is the highest for chiral center and decreases with increasing distance from the chiral center. In other words, the $\Delta\varepsilon/\varepsilon$ values of selected vibrations referred to the $\Delta\varepsilon/\varepsilon$ value of chiral center, relative $\Delta\varepsilon/\varepsilon$ values represent the transfer of asymmetry from chiral center to the rest of molecule. Dissymmetry factors of **6** (Fig. 5A) and **14** (Fig. 5B) were calculated for characteristic vibrations of methanodiazocin bridge, C═O, and methyl groups, which are located in the chiral center and in a different distance from the chiral core.

The maximal $\Delta\varepsilon/\varepsilon$ value was observed for the C–N stretching vibrations of the chiral methanodiazocin bridge (9) in the spectra of **6** and **14**, as expected. The $\Delta\varepsilon/\varepsilon$ values of C═O stretch (1) and CH_3 symmetrical bend (6) of **6** are almost the same and reach about one quarter of the $\Delta\varepsilon/\varepsilon$ value of methanodiazocin bridge (9). For dimer **14**, the $\Delta\varepsilon/\varepsilon$ value of amide I stretch (1) and the CH_3 symmetrical bend (6) are given by summation[†] of contributions of individual amide I and methyl groups, respectively. Both values, therefore, represent the average of individual contributions. They reach only one fifth of the $\Delta\varepsilon/\varepsilon$ value of methanodiazocin bridge (9).

The transfer of asymmetry from methanodiazocin bridge to the *N*-methylpyrrole tripeptide arms of **14** can be clarified by comparing the relative $\Delta\varepsilon/\varepsilon$ values of C═O stretch (1) and CH_3 symmetrical bend (6) referred to the $\Delta\varepsilon/\varepsilon$ value of band no. 9 for **14** versus the same values obtained for **6**. There are two possible extreme situations. Firstly, the asymmetry in **14** is transferred only to the first amide group of the tripeptidic arms, then the decrease of *relative* $\Delta\varepsilon/\varepsilon$ values (1 and 6) of **14** versus **6** should be approximately 80%. Secondly, the asymmetry in **14** is transferred to all amide groups of tripeptidic arms equally, then the *relative* $\Delta\varepsilon/\varepsilon$ values (1 and 6) should be the same for **6** and **14**. The approximately 20% reduction of *relative* $\Delta\varepsilon/\varepsilon$ values (1 and 6) of **14** compared to **6** indicates a descending but important influence of the chiral methanodiazocin bridge on the optical activity in the *N*-methylpyrrole tripeptidic arms of **14**. On the other hand, partially differentiated vibrations of the *N*-methylpyrrole units of **14** (2a, 2b, 2c and 2d), showing only one VCD signal for *N*-methylpyrroles of the central core (2c) of **14**, is not consistent with the distribution of asymmetry far from the di-*N*-methylpyrrolomethanodiazocin core.

In summary, the asymmetry in both **6** and **14** is definitely transported up to the carboxyl and first amide, respectively. Distribution of asymmetry to the rest of dimer **14** is then ambiguous.

[†] The IR and VCD signals of all present amide groups as well as methyl groups are not resolved and are given by summation of all appropriate signals. This is evident from different ratio between the IR signal intensity of the methyl groups and the methanodiazocin bridge in the spectra of **6** and **14**. While the IR signal of **6** at 1376 cm^{-1} is as intensive as the IR signal of **6** at 1201 cm^{-1} and the IR signal of **14** at 1376 cm^{-1} is three times more intense than IR signal of **14** at 1201 cm^{-1}.

2.3. Binding study

DNA binding activity of dimers **11**–**14** was assayed on DNAs by NMR and ECD spectroscopies, and using a fluorescence probe displacement assay in deutero-water and deutero-water/deutero-methanol mixture (2:1), and cacodylate buffer, respectively.

NMR experiments were only performed with **11** and **12**, because the solubility of the other dimers (**13** and **14**) is limited and these dimers form aggregates in water as well as in the mixture of water and methanol. Addition of calf thymus (ct) DNA to the solution of **11** led to distension (line broadening) of all signals of **11** in ^{1}H spectrum. The presence of ct-DNA has the biggest influence on the signals of methylene protons of methanodiazocin bridge. Distension of signals of **11** indicates an intermediate rate of exchange between the complexed and free state of **11**. In addition, the hydrogen nuclei of **11** relaxed faster in the presence of ct-DNA. Generally, shorter relaxation times signify a decrease in the degree of freedom of molecules, which is consistent with the complex formation of **11** and ct-DNA. The same results were achieved for dimer **12** at considerable (approximately 10 times) lower ratio of ct-DNA and ligand.

On the other hand, dimers **11** and **12** did not provide the induced ECD band above 300 nm upon their addition to ct-DNA (see Fig. 6) that is typical for binding of **1** and its analogues to minor groove of ct-DNA.[55,56] In addition, the intensity of the induced ECD band is proportional to the strength of binding. In the presence of ct-DNA, only dimers **13** and **14** provided new ECD bands above 300 nm. The magnitude of the positive ECD band was more than three times higher in the case of dimer **14** compared to **13**. These results are in agreement with the previous observation that the strength of binding of distamycin related compounds

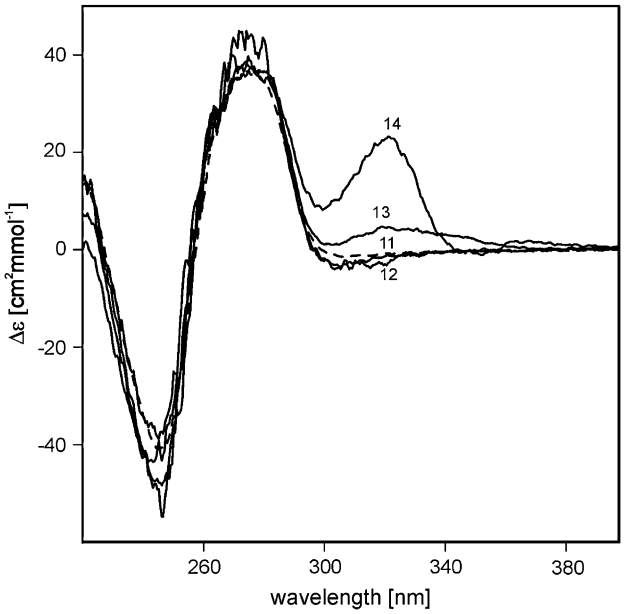

Figure 6. ECD spectra of **11–14** in the presence of ct-DNA (solid lines) and the spectrum of pure ct-DNA (dashed line).

to DNA increases with the number of *N*-methylpyrrole units present in the oligopeptides.[20]

The ECD signal of ct-DNA, the positive and negative bands at 274 and 245 nm, is typical for the B-form of DNA[57] and did not change on adding dimer **11**–**14** to ct-DNA (see Fig. 6). So, the interaction between B-DNA and **13**, and **14** does not significantly influence the structure of ct-DNA.

The following ECD spectroscopic measurements were done for the interactions of dimer **12**–**14** with poly(dA-dT)$_2$ and poly(dC-dG)$_2$, respectively. As expected, **13**-poly(dA-dT)$_2$ and **14**-poly(dA-dT)$_2$ exhibited the induced ECD band above 300 nm. In addition, dramatic changes in the induced ECD band of **14**-poly(dA-dT)$_2$ were observed at higher drug concentration (c(**14**):c(poly(dA-dT)$_2$), ~1:4). This indicates a two-step binding mode of **14** to poly(dA-dT)$_2$. The intensity of the induced ECD band in the spectrum of **12**-poly(dA-dT)$_2$ and **14**-poly(dC-dG)$_2$ was low and reached less than one sixth of the intensity of ECD band corresponding to **13**-poly(dA-dT)$_2$ or **14**-poly(dA-dT)$_2$. The addition of **12** and **13** to the poly(dC-dG)$_2$ did not lead to induction of the ECD band above 300 nm.

The binding stoichiometry (n_b, number of dimer molecules bound per nucleotide base pair) of **14** to ct-DNA and poly(dA-dT)$_2$ was determined by ECD spectral titrations of DNA with **14**. The n_b was determined as n (the ratio of c(**14**) to c(DNA)) at the break in the plot of the intensity of the induced ECD signal at selected wavelength against the n. The n_b values (~0.15 for ct-DNA and ~0.12 for poly(dA-dT)$_2$) indicate that DNA saturates at about one molecule of **14** per six nucleotide base pairs in the case of ct-DNA and one molecule of **14** per about eight nucleotide base pairs in the case of poly(dA-dT)$_2$. The number of base pairs bonded by dimer **14** is lower than one would expect for bidentate binding mode of such compound to DNA. In addition, a similar n_b value was previously obtained for the interaction of **1** with poly(dA-dT)$_2$.[28] It appears that dimers **12**–**14** bind to DNA either through one of their *N*-methylpyrrole peptide arms and partial contacts of the linker or through the terminal segments of both *N*-methylpyrrole peptide arms only.

The quantification of binding strength of dimers **12**–**14** to DNA was done by the competition between compounds **1**, **12**–**14**, and ethidium bromide (EB).[58] Displacement of ethidium bromide from ct-DNA, poly(dA-dT)$_2$, and poly(dC-dG)$_2$ was accompanied by a decrease in the fluorescence intensity measured at 595 nm. The apparent binding constants (K_{app}) were calculated from K_{EB}[EB]=K_{app}[drug], where [drug] is the concentration of **12**–**14** at a 50% reduction of fluorescence and K_{EB} is known.[59] The K_{app} values for **1** are close to the data obtained by previous measurements.[27,60] The K_{app} values for **12**–**14** calculated by this way (see Table 2) are consistent with the results obtained by ECD spectroscopy. The almost identical K_{app} values of **12** to all types of studied DNAs show that dimer **12** binds DNA without any selectivity. Dimers **13** and **14** showed lower affinity for ct-DNA and poly(dA-dT)$_2$ than **1**, however, they bound significantly stronger to poly(dC-dG)$_2$. Nevertheless, both compounds exhibit a preference for AT sequences compared to GC sequences. The strength

Table 2. Apparent binding constants, K_{app} ($\times 10^5$ M^{-1})

Compound	ct-DNA	poly(dA-dT)$_2$	poly(dC-dG)$_2$	poly(dA-dT)$_2$/ poly(dC-dG)$_2$
1	140±4	346±3	2.0±0.2	173
12	2.0±0.5	2.4±0.5	1.8±0.4	—
13	33±3	34±4	20±2	1.7
14	99±4	148±4	40±3	3.7
(4*R*,9*R*)-**14**	112±4	191±4	42±3	4.5
(4*S*,9*S*)-**14**	90±3	128±3	36±2	3.5

of binding to DNAs and the preference for AT sequences increases with the increasing number of pyrrole units in the dimer. A decrease in the binding affinity and selectivity of methanodiazocin linked distamycin analogues compared to distamycin itself confirms the conclusion from the binding stoichiometry determination, the nonbidentate binding of dimers **12**–**14** to DNA. On the other hand, distamycin A and netropsin exhibit higher binding affinity for ct-DNA than 'head-to-head' bisnetropsin analogues with a 1,2-cyclopropanedicaraboxamide linker that binds to DNA with a bidentate binding mode.[28] Nevertheless, all the data evaluation indicates that the rigid methanodiazocin bridge is not an optimal spacer molecule for the construction of bidentate minor groove binders based on 'head-to-head' bisdistamycin derivatives.

The stereochemical control of minor groove binding by the methanodiazocin bridge on *N*-methylpyrrole oligopeptide dimer was studied with the optically pure forms of the most effective binding dimer **14**. The ECD spectral titrations suggested a similar affinity of (4*R*,9*R*)-**14** and (4*S*,9*S*)-**14** to all studied DNAs. The ECD spectra of (4*R*,9*R*)-**14**-poly(dC-dG)$_2$ and (4*S*,9*S*)-**14**-poly(dC-dG)$_2$ after subtraction of poly(dC-dG)$_2$ contributions were nearly symmetrical (mirror-image) with respect to base lines. This 'spectral symmetry' explains the small intensity of the ECD band above 300 nm at titration of poly(dC-dG)$_2$ with racemic **14**. Fluorescence probe displacement assay shows that enantiomer (4*R*,9*R*)-**14** has a slightly higher affinity for all studied DNAs than enantiomer (4*S*,9*S*)-**14** (Table 2). In addition, enantiomer (4*R*,9*R*)-**14** also exhibited slightly higher discrimination for poly(dA-dT)$_2$ versus poly(dC-dG)$_2$ sequences than enantiomer (4*S*,9*S*)-**14**. The '*R* enantiomeric discrimination' has also been described by Lown and co-workers on a netropsin dimer linked by *trans*-1,2-cyclopropane.[29]

3. Conclusion

We have described new bisdistamycin analogues with a TB scaffold in racemic as well as chiral fashion. DNA binding studies of such compounds showed that the 'head-to-head' linking of two *N*-methylpyrrole oligopeptides by the methanodiazocin scaffold caused decreasing affinity and selectivity of binding to AT sequences, and increases affinity to CG sequences compared to distamycin A. Moreover, the directionality in the binding can be controlled by the stereochemistry of our linker. In the case of the most effective binding dimer **14**, the (4*R*,9*R*)-form is better suited for interaction with all studied DNAs than the (4*S*,9*S*)-form.

4. Experimental

4.1. General

Thin-layer chromatography was performed on Merck Silica gel 60 F_{254} TLC plates. For column chromatography the neutral silica gel SiliTech 32–63, 60 Å (ICN Biomedicals) was used. ^{1}H, ^{13}C, 1D NOESY, gHSQC, gHMBC, and gCOSY NMR spectra were obtained with Varian Gemini 300 HC (300.1 MHz for ^{1}H NMR and 75.5 MHz for ^{13}C NMR spectra) at 23 °C in $CDCl_3$ or $(CD_3)_2SO$. Correlation NMR techniques were applied for the assignment of chemical shifts to atoms of the molecules. The chemical shifts are given in parts per million relative to $(CH_3)_4Si$. For the sake of clarity in the assignment of NMR spectra, the pyrrole rings of the dimer **12**–**14** are numbered from methanodiazocin bridge to *N*,*N*-dimethylaminopropyl terminal. Mass spectra were recorded with a VG Analytical ZAB-EQ spectrometer and Biflex mass spectrometer (MALDI-MS).

Calf thymus DNA (42% C+G, mean molecular mass ~20 MDa) was prepared and characterized as described previously.[61] Homopolymers poly(dA-dT)$_2$ and poly(dC-dG)$_2$ were purchased from Sigma. The DNA concentrations are expressed per base pairs.

The ECD spectra were measured at a resolution of 1 nm using Jasco-810 spectrophotometer using 0.1 cm path length and three accumulations. The concentration of **11**–**14** was 0.2 mM. The DNA concentration was 1.6 mM. Cacodylate/NaCl (0.02/0.1 M) buffer of pH 7.4 was used as a solvent.

Fluorescence measurements were performed on a Shimadzu RF 40 spectrofluorophotometer using a 1 cm quartz cell at room temperature. The DNA–EB complexes were excited at 546 nm and the fluorescence was measured at 595 nm. To the solution of EB and DNA (10 mM Tris pH 7.4, 1 mM EDTA, 1.3 μM EB, and 3.9 μM DNA) were added aliquots of a 1 mM stock solution of **12**–**14** and the fluorescence was measured after each addition until the fluorescence was reduced to 50%.

The VCD and IR absorption spectra were measured at a resolution of 4 cm^{-1} using Bruker FTIR IFS 66/S spectrometer equipped with a VCD/IRRAS module PMA 37.[62] Demountable cell composed of 50 μm Teflon spacer and CaF_2 windows were used. VCD spectra were obtained as the average of 25 blocks of scans, each block counts 3680 scans (20 min). Concentrations of **6** and **14** were 0.16 and 0.04 M ($(CD_3)_2SO$), respectively. The concentration was chosen so that the absorbance maxima did not exceed value of about 0.8 for 50 μm path length in the spectral region 1800–1100 cm^{-1}.

4.2. Benzyl 1-methyl-4-nitropyrrole-2-carboxylate (3)

To a solution of 1-methyl-4-nitro-2-trichloroacetylpyrrole (30.02 g, 110.57 mmol) in THF (160 ml), a mixture of benzyl alcohol (30 ml, 290 mmol) and natrium hydride (0.50 g, 21.7 mmol) in THF (40 ml) was added at 0 °C. The resulting suspension was warmed to room temperature and stirred overnight. The reaction mixture was neutralized with $TsOH \cdot H_2O$ (yellow color changed to white) and the

insoluble part was filtered off. The filtrate was concentrated in vacuo and the residue was diluted with petroleum ether (300 ml), which caused crystallization of **3**. Pale yellow crystals of product **3** (25.12 g, 87%) were filtered off, washed with petrolether (3×100 ml), cold methanol (2×50 ml), water (2×50 ml) and again with methanol (2×50 ml), and dried in vacuo.

Mp 109–111 °C (lit.[40] mp 112–113 °C); ^{1}H NMR ($CDCl_3$) δ 3.97 (3H, s, NCH_3), 5.29 (2H, s, CH_2), 7.32–7.43 (5H, m, C*H*-Ph), 7.44 (1H, d, *J*=2.2, C*H*CCO), 7.59 (1H, d, *J*=2.2, C*H*NCH$_3$); ^{13}C NMR ($CDCl_3$) δ 37.83 (N*C*H$_3$), 66.38 (*C*H$_2$), 112.76 (*C*HCCO), 128.05 (*o*-*C*H of Ph), 122.68 (*C*CO), 127.66 (*C*HNCH$_3$), 128.34 (*p*-*C*H of Ph), 128.55 (*m*-*C*H of Ph), 135.09 (*C*NO$_2$), 135.31 (*ipso*-*C* of Ph), 159.36 (*C*O).

4.3. Benzyl 1-methyl-4-aminopyrrole-2-carboxylate hydrochloride (4)

Freshly prepared nickel boride Ni_2B (15.00 g) and **3** (15.00 g, 57.63 mmol) were added to methanol (390 ml) and 1 M hydrochloric acid (130 ml). The resulting suspension was stirred at 70 °C till **3** was no longer present in the reaction mixture (followed by TLC). For each 1 h, 2 ml of concd hydrochloric acid were slowly added to the reaction mixture. The reaction mixture was filtered and the filter cake was washed with methanol (3×50 ml). All liquid portions were combined and concentrated in vacuo to 100 ml (mainly to remove methanol), which caused crystallization of **4** (10.52 g, 68%) as pale brown crystals. A second crop of product **4** (3.64 g, 24%) was obtained by concentration of mother liquor.

Mp 213–217 °C (decomp.); ^{1}H NMR ((CD$_3$)$_2$SO) δ 3.84 (3H, s, NCH_3), 5.23 (2H, s, CH_2), 6.83 (1H, d, *J*=2.2, C*H*CCO), 7.27 (1H, d, *J*=2.2, C*H*NCH$_3$), 7.28–7.42 (5H, m, C*H*-Ph), 10.25 (3H, br s, $^+$NH_3); ^{13}C NMR ((CD$_3$)$_2$SO) δ 36.50 (N*C*H$_3$), 65.15 (*C*H$_2$), 111.63 (*C*HCCO), 113.88 (*C*NH$_3$), 120.56 (*C*CO), 123.97 (*C*HNCH$_3$), 127.76 (*o*-*C*H of Ph), 127.96 (*p*-*C*H of Ph), 128.40 (*m*-*C*H of Ph), 136.13 (*ipso*-*C* of Ph), 159.36 (*C*O); MS (FAB) *m*/*z* (%): 231 (100) [M$^+$−Cl], 243 (10) [M$^+$−HCl+Na].

4.4. Dibenzyl-4,9-methano-1,6-dimethyl-4,5,9,10-tetrahydro-1*H*,6*H*-dipyrrolo-[3,2-*b*:3′,2′-*f*][1,5]diazocin-2,7-dicarboxylate (5)

Hydrochloride **4** (5.00 g, 18.75 mmol) was dissolved in ethanol (50 ml), and then formaldehyde (7.5 ml, 36% aqueous solution) and concd HCl (7.5 ml) were added. The reaction mixture was stirred for 24 h at room temperature and then concentrated under reduced pressure to one half of the original volume, diluted with water (100 ml), and finally basified with ammonia solution. The basic mixture (pH 14) was extracted with dichloromethane (3×50 ml) and the combined organic layers were dried over anhydrous $MgSO_4$ and evaporated to dryness. The residue was crystallized (dichloromethane/diethyl ether) to give benzyl ester **5** (2.75 g, 59%) as colorless crystals.

Mp 182–185 °C; ^{1}H NMR ($CDCl_3$) δ 3.64 (6H, s, NCH_3), 3.92 (2H, d, *J*=15.9, *endo* C*H*HN), 4.09 (2H, s, NCH_2N), 4.36 (2H, d, *J*=16.5, *exo* CH*H*N), 5.24 (4H, s, CH_2Ph), 6.77 (2H, s, C*H*CCO), 7.36 (10H, m, C*H*-Ph); ^{13}C NMR ($CDCl_3$) δ 32.56 (N*C*H$_3$), 52.21 (C*C*H$_2$N), 65.31 (*C*H$_2$Ph), 68.90 (N*C*H$_2$N), 110.29 (*C*HCCO), 119.76 (*C*CO), 127.18 (*C*CH$_2$N), 127.86 (*o*-*C*H of Ph), 127.97 (*p*-*C*H of Ph), 128.46 (*m*-*C*H of Ph), 131.24 (*C*NCH$_2$), 136.50 (*ipso*-*C* of Ph), 160.90 (*C*O).

4.5. 4,9-Methano-1,6-dimethyl-4,5,9,10-tetrahydro-1*H*,6*H*-dipyrrolo-[3,2-*b*:3′,2′-*f*][1,5]diazocin-2,7-dicarboxylic acid (6)

To a solution of benzyl ester **5** (0.490 g, 0.99 mmol) in dry DMF (15 ml), a catalyst (5% Pd/C, 50 mg) was added. The reaction mixture was treated under hydrogen atmosphere (101.3 kPa) at room temperature for 3 h. The catalyst was filtered off and the filtrate was evaporated in vacuo to dryness. Brownish residue was stirred with methanol (3 ml) for 3 h and the mixture was then filtered to give acid **6** (275 mg, 88% yield) as a white powder.

Mp>200 °C (decomp.); ^{1}H NMR ((CD$_3$)$_2$SO) δ 3.56 (6H, s, NCH_3), 3.89 (2H, d, *J*=16.6, *endo* C*H*HN), 3.94 (2H, s, NCH_2N), 4.27 (2H, d, *J*=16.5, *exo* CH*H*N), 6.53 (2H, s, C*H*CCO); ^{13}C NMR ((CD$_3$)$_2$SO) δ 32.82 (N*C*H$_3$), 51.52 (C*C*H$_2$N), 68.28 (N*C*H$_2$N), 109.67 (*C*HCCO), 119.59 (*C*CO), 127.23 (*C*CH$_2$N), 130.95 (*C*NCH$_2$), 162.11 (*C*O); MS (FAB) *m*/*z* (%): 317 (100) [M$^+$+H]; elemental analysis calcd (%) for $C_{15}H_{16}N_4O_4$ (316.32): C 56.96, H 5.10, N 17.71; found: C 56.87, H 5.51, N 17.81.

4.6. Bis(benzotriazol-1-yl)-4,9-methano-1,6-dimethyl-4,5,9,10-tetrahydro-1*H*,6*H*-dipyrrolo-[3,2-*b*:3′,2′-*f*]-[1,5]diazocin-2,7-dicarboxylate (2)

A solution of acid **6** (100 mg, 0.32 mmol) with HOBt (120 mg, 0.889 mmol) and DCC (165 mg, 0.800 mmol) in dichloromethane (15 ml) and DMF (2 ml) was stirred for 12 h at room temperature. The insoluble part was filtered off and the filtrate was evaporated. The residue was chromatographed on silica (gradient from dichloromethane/diethyl ether 7:3 to diethyl ether) to give active ester **2** (115 mg, 66%), which was further purified by precipitation (dichloromethane/diethyl ether).

Mp>220 °C (decomp.); ^{1}H NMR ($CDCl_3$) δ 3.70 (6H, s, NCH_3), 4.09 (2H, d, *J*=16.8, *endo* C*H*HN), 4.20 (2H, s, NCH_2N), 4.51 (2H, d, *J*=16.8, *exo* CH*H*N), 7.22 (2H, s, C*H*CCO), 7.36–7.58 (6H, m, C*H*-Ar), 8.06 (2H, d, *J*=8.3, C*H*CNO); ^{13}C NMR ($CDCl_3$) δ 32.94 (N*C*H$_3$), 52.60 (C*C*H$_2$N), 68.77 (N*C*H$_2$N), 108.30 (*C*HCHCNN), 113.16 (*C*HCCO), 113.86 (*C*CO), 120.35 (*C*HCNO), 124.61 (*C*HCHCNO), 128.48 (*C*HCHCNN), 128.95 (*C*NN), 131.47 (*C*CH$_2$N), 132.51 (*C*CH$_2$N), 143.32 (*C*NO), 156.50 (CO); MS (FAB) *m*/*z* (%): 551 (65) [M$^+$+H], 416 (100) [M$^+$−C$_6$H$_4$N$_3$O]; elemental analysis calcd (%) for $C_{27}H_{22}N_{10}O_4$ (550.54): C 58.91, H 4.03, N 25.44; found: C 58.82, H 4.18, N 25.30.

4.6.1. Compound (4*R*,9*R*)-2. 1-Phenylethyl ester (*R*)(4*R*,9*R*)(*R*)-**15a** (504 mg, 0.961 mmol) was dissolved in DMF (10 ml), and then TEA (600 μl) and catalyst (5% Pd/C, 97 mg) were added. The reaction mixture was treated

under hydrogen atmosphere (101.3 kPa) at room temperature for 3 h. The catalyst was filtered off and the filtrate was diluted with dichloromethane (50 ml), and then HOBt (600 mg, 4.445 mmol) and DCC (800 mg, 3.879 mmol) were added. The reaction mixture was stirred for 12 h at room temperature and then evaporated in vacuo to dryness. Dichloromethane (15 ml) was added to the residue and the insoluble part was filtered off. Filtrate was chromatographed on silica (gradient from dichloromethane/diethyl ether 7:3 to diethyl ether) to give active ester (4*R*,9*R*)-**2** (400 mg, 83%), which was further purified by precipitation (dichloromethane/diethyl ether).

Compound (4*R*,9*R*)-**2** has identical NMR spectra as **2**; $[\alpha]_D^{20}$ +62 (*c* 0.156 g/100 ml DMF).

4.6.2. Compound (4*S*,9*S*)-2. Enantiomer (4*S*,9*S*)-**2** was prepared by the same synthetic procedure as (4*R*,9*R*)-**2**. Reduction of **15b** (200 mg, 17.3 mmol) by 5% Pd/C (40 mg) followed by reaction with HOBt (240 mg, 1.778 mmol) and DCC (320 mg, 1.551 mmol) gave active ester (4*S*,9*S*)-**2** (150 mg, 78%).

Compound (4*S*,9*S*)-**2** has identical NMR spectra as **2**; $[\alpha]_D^{20}$ –59 (*c* 0.409 g/100 ml DMF).

4.7. *N*,*N*′-Bis(dimethylaminopropan-3-yl)-4,9-methano-1,6-dimethyl-4,5,9,10-tetrahydro-1*H*,6*H*-dipyrrolo-[3,2-*b*:3′,2′-*f*][1,5]diazocin-2,7-dicarboxamide (11)

N,*N*-Dimethyl-propane-1,3-diamine **7** (2 ml) was added to a DMF (3 ml) solution of TB active ester (150 mg, 272 μmol) and the mixture was stirred for 5 h at room temperature. The reaction mixture was evaporated to dryness in vacuo and the residue was separated by column chromatography (concd aqueous ammonia/methanol 5:95) to give desired amide **11** (120 mg, 91%) as white powder.

Mp>220 °C (decomp.); ν_{max} (KBr)/cm^{-1} 3350 (NH), 1629 (C═O), 1560 and 1535 (pyrrole, ring vib.), and 1198 (C–N); ^{1}H NMR ((CD$_3$)$_2$SO) δ 1.55 (4H, quintet, *J*=7.2, C*H*$_2$CH$_2$N), 2.12 (12H, s, N(C*H*$_3$)$_2$), 2.23 (4H, t, *J*=7.2, CH$_2$C*H*$_2$N), 3.12 (4H, m, C*H*$_2$NH), 3.52 (6H, s, NC*H*$_3$), 3.75 (2H, d, *J*=16.2, *endo* C*H*HN), 3.89 (2H, s, NC*H*$_2$N), 4.25 (2H, d, *J*=16.2, *exo* CH*H*N), 6.46 (2H, s, C*H*CCO), 7.84 (2H, t, *J*=5.6, N*H*); ^{13}C NMR ((CD$_3$)$_2$SO) δ 27.17 (*C*H$_2$CH$_2$N), 32.03 (NCH$_3$), 36.78 (*C*H$_2$NH), 45.00 (N(*C*H$_3$)$_2$), 51.40 (C*C*H$_2$N), 56.80 (CH$_2$*C*H$_2$N), 68.47 (N*C*H$_2$N), 104.75 (*C*HCCO), 122.84 (*C*CO), 124.24 (*C*CH$_2$N), 130.39 (*C*NCH$_2$), 161.36 (*C*O); MS (FAB) *m*/*z* (%): 485 (100) [M$^+$+H]; elemental analysis calcd (%) for C$_{25}$H$_{40}$N$_8$O$_2$ (484.65): C 61.96, H 8.32, N 23.12; found: C 61.79, H 8.38, N 23.03.

4.8. General protocol for the preparation of dimers 12–14

The solution of amine (**8**–**10**) and TB active ester **2** in DMF was stirred for 12 h at 60 °C. The reaction mixture was evaporated to dryness in vacuo and the residue was separated by column chromatography (concd aqueous ammonia/methanol 5:95) to give corresponding TB distamycin dimer (**12**–**14**).

4.9. *N*,*N*′-Bis(5-[3-dimethylaminopropyl]aminocarbonyl-1-methylpyrrol-3-yl)-4,9-methano-1,6-dimethyl-4,5,9,10-tetrahydro-1*H*,6*H*-dipyrrolo-[3,2-*b*:3′,2′-*f*]-[1,5]diazocin-2,7-dicarboxamide (12)

Reaction of amine **8** (176 mg, 787 μmol) with active ester **2** (170 mg, 309 μmol) gave dimer **12** (150 mg, 67%) as a light yellow powder.

ν_{max} (KBr)/cm^{-1} 3400 (NH), 1636 (C═O), 1578 and 1533 (pyrrole, ring vib.), and 1198 (C–N); ^{1}H NMR ((CD$_3$)$_2$SO) δ 1.59 (4H, quintet, *J*=6.9, C*H*$_2$CH$_2$N), 2.15 (12H, s, N(C*H*$_3$)$_2$), 2.26 (4H, t, *J*=6.6, CH$_2$C*H*$_2$N), 3.16 (4H, q, *J*=6.2, C*H*$_2$NH), 3.58 (6H, s, NC*H*$_3$-Py$_0$), 3.76 (3H, s, NC*H*$_3$-Py$_1$), 3.83 (2H, d, *J*=16.2, *endo* C*H*HN), 3.95 (2H, s, NC*H*$_2$N), 4.32 (2H, d, *J*=16.2, *exo* CH*H*N), 6.68 (2H, s, C*H*CCO-Py$_0$), 6.76 (2H, d, *J*=1.9, C*H*CCO-Py$_1$), 7.12 (2H, d, *J*=1.7, C*H*NCH$_3$-Py$_1$), 8.06 (2H, t, *J*=5.6, CON*H*-Py$_1$), 9.65 (2H, s, CON*H*-Py$_0$); ^{13}C NMR ((CD$_3$)$_2$SO) δ 27.02 (*C*H$_2$CH$_2$N), 32.18 (N*C*H$_3$-Py$_0$), 35.95 (N*C*H$_3$-Py$_1$), 37.00 (*C*H$_2$NH), 45.01 (N(*C*H$_3$)$_2$), 51.52 (C*C*H$_2$N), 56.95 (CH$_2$*C*H$_2$N), 68.50 (N*C*H$_2$N), 103.91 (*C*HCCO-Py$_1$), 105.52 (*C*HCCO-Py$_0$), 117.64 (*C*HNCH$_3$), 122.11 (*C*NH-Py$_1$), 122.65 (*C*CO-Py$_0$), 123.01 (*C*CO-Py$_1$), 125.00 (*C*CH$_2$N), 130.56 (*C*NCH$_2$), 158.60 (*C*O-Py$_0$), 161.21 (*C*O-Py$_1$); MS (MALDI) *m*/*z* (%): 729 (100) [M$^+$+H]; elemental analysis calcd (%) for C$_{37}$H$_{52}$N$_{12}$O$_4$ (728.90): C 60.97, H 7.19, N 23.06; found: C 60.84, H 7.27, N 23.02.

4.10. *N*,*N*′-Bis(5-[{5-(3-dimethylaminopropyl)aminocarbonyl-1-methylpyrrol-3-yl}aminocarbonyl]-1-methylpyrrol-3-yl)-4,9-methano-1,6-dimethyl-4,5,9,10-tetrahydro-1*H*,6*H*-dipyrrolo-[3,2-*b*:3′,2′-*f*][1,5]diazocin-2,7-dicarboxamide (13)

Reaction of amine **9** (138 mg, 398 μmol) with active ester **2** (90 mg, 163 μmol) gave dimer **13** (105 mg, 66%) as a yellow powder.

ν_{max} (KBr)/cm^{-1} 3400 (NH), 1640 (C═O), 1581 and 1531 (pyrrole, ring vib.), and 1198 (C–N); ^{1}H NMR ((CD$_3$)$_2$SO) δ 1.60 (4H, quintet, *J*=7.0, C*H*$_2$CH$_2$N), 2.16 (12H, s, N(C*H*$_3$)$_2$), 2.27 (4H, t, *J*=7.0, CH$_2$C*H*$_2$N), 3.17 (4H, m, C*H*$_2$NH), 3.60 (6H, s, NC*H*$_3$-Py$_0$), 3.77 (6H, s, NC*H*$_3$-Py$_2$), 3.81 (6H, s, NC*H*$_3$-Py$_1$), 3.85 (2H, d, *J*=16.5, *endo* C*H*HN), 3.96 (2H, s, NC*H*$_2$N), 4.34 (2H, d, *J*=16.0, *exo* CH*H*N), 6.69 (2H, s, C*H*CCO-Py$_0$), 6.81 (2H, d, *J*=1.8, C*H*CCO-Py$_2$), 6.98 (2H, d, *J*=1.8, C*H*CCO-Py$_1$), 7.16 (2H, d, *J*=1.8, C*H*NCH$_3$-Py$_2$), 7.18 (2H, d, *J*=1.8, C*H*NCH$_3$-Py$_1$), 8.07 (2H, t, *J*=5.5, CON*H*-Py$_2$), 9.72 (2H, s, CON*H*-Py$_0$), 9.87 (2H, s, CON*H*-Py$_1$); ^{13}C NMR ((CD$_3$)$_2$SO) δ 26.98 (*C*H$_2$CH$_2$N), 32.22 (N*C*H$_3$-Py$_0$), 35.97 (N*C*H$_3$-Py$_2$), 36.10 (N*C*H$_3$-Py$_1$), 36.99 (*C*H$_2$NH), 44.96 (N(*C*H$_3$)$_2$), 51.55 (C*C*H$_2$N), 56.92 (CH$_2$*C*H$_2$N), 68.52 (N*C*H$_2$N), 104.03 (*C*HCCO-Py$_2$), 104.58 (*C*HCCO-Py$_1$), 105.57 (*C*HCCO-Py$_0$), 117.77 (*C*HNCH$_3$-Py$_2$), 118.31 (*C*HNCH$_3$-Py$_1$), 122.15 (*C*NH-Py$_1$+Py$_2$), 122.64 (*C*CO-Py$_0$), 122.79 (*C*CO-Py$_1$), 122.99 (*C*CO-Py$_2$), 125.07 (*C*CH$_2$N), 130.59 (*C*NCH$_2$), 158.46 (CO-Py$_1$), 158.65 (CO-Py$_0$), 161.23 (*C*O-Py$_2$); MS (MALDI) *m*/*z* (%): 973 (100) [M$^+$+H], 995 (10) [M$^+$+Na]; elemental analysis calcd (%) for C$_{49}$H$_{64}$N$_{16}$O$_6$ (973.16): C 60.48, H 6.63, N 23.03; found: C 60.37, H 6.72, N 23.00.

4.11. *N*,*N*′-Bis(5-[{5-[{5-(3-dimethylaminopropyl)-aminocarbonyl-1-methylpyrrol-3-yl}aminocarbonyl]-1-methylpyrrol-3-yl}aminocarbonyl]-1-methylpyrrol-3-yl)-4,9-methano-1,6-dimethyl-4,5,9,10-tetrahydro-1*H*,6*H*-dipyrrolo-[3,2-*b*:3′,2′-*f*][1,5]diazocin-2,7-dicarboxamide (14)

Reaction of amine **10** (310 mg, 662 μmol) with active ester **2** (150 mg, 272 μmol) gave dimer **14** (106 mg, 39%) as a yellow powder.

ν_{max} (KBr)/cm^{-1} 3400 (NH), 1640 (C═O), 1581 and 1531 (pyrrole, ring vib.), and 1198 (C–N); ^{1}H NMR ((CD$_3$)$_2$SO) δ 1.63 (4H, quintet, J=6.9, CH_2CH$_2$N), 2.22 (12H, s, N(CH_3)$_2$), 2.35 (4H, t, J=6.9, CH$_2$CH_2N), 3.19 (4H, m, CH_2NH), 3.62 (6H, s, NCH_3-Py$_0$), 3.80 (6H, s, NCH_3-Py$_3$), 3.87 (14H, m, 2×NCH_3-(Py$_1$+Py$_2$)+*endo* CHHN), 3.98 (2H, s, NCH_2N), 4.36 (2H, d, J=16.0, *exo* CHHN), 6.72 (2H, s, CHCCO-Py$_0$), 6.84 (2H, s, CHCCO-Py$_3$), 7.01 (2H, s, CHCCO-Py$_1$), 7.04 (2H, s, CHCCO-Py$_2$), 7.18 (2H, s, CHNCH$_3$-Py$_3$), 7.20 (2H, s, CHNCH$_3$-Py$_2$), 7.23 (2H, s, CHNCH$_3$-Py$_1$), 8.08 (2H, t, J=5.1, CONH-Py$_3$), 9.73 (2H, s, CONH-Py$_0$), 9.89 (2H, s, CONH-Py$_2$), 9.94 (2H, s, CONH-Py$_1$); ^{13}C NMR ((CD$_3$)$_2$SO) δ 26.78 (CH_2CH$_2$N), 32.21 (NCH$_3$-Py$_0$), 35.96 (NCH$_3$-Py$_3$), 36.10 (NCH$_3$-Py$_1$+Py$_2$), 36.84 (CH$_2$NH), 44.73 (N(CH$_3$)$_2$), 51.53 (CCH$_2$N), 56.73 (CH$_2$CH$_2$N), 68.53 (NCH$_2$N), 104.09 (CHCCO-Py$_3$), 104.64 (CHCCO-Py$_{1\ or\ 2}$), 104.71 (CHCCO-Py$_{1\ or\ 2}$), 105.58 (CHCCO-Py$_0$), 117.81 (CHNCH$_3$-Py$_3$), 118.36 (CHNCH$_3$-Py$_2$), 118.43 (CHNCH$_3$-Py$_1$), 122.17 (CNH-Py$_{1-3}$+Py$_{1-3}$), 122.20 (CNH-Py$_{1-3}$), 122.63 (CCO-Py$_0$), 122.77 (CCO-Py$_1$+Py$_2$), 122.95 (CCO-Py$_3$), 125.07 (CCH$_2$N), 130.58 (CNCH$_2$), 158.48 (CO-Py$_{1\ or\ 2}$), 158.51 (CO-Py$_{1\ or\ 2}$), 158.65 (CO-Py$_0$), 161.27 (CO-Py$_3$); MS (MALDI) *m*/*z* (%): 1217 (100) [M$^+$+H], 615 (90) [M$^+$-C$_{31}$H$_{39}$N$_9$O$_4$]; elemental analysis calcd (%) for C$_{61}$H$_{76}$N$_{20}$O$_8$ (1217.42): C 60.18, H 6.29, N 23.01; found: C 60.04, H 6.34, N 22.84.

4.11.1. Compound (4*R*,9*R*)-14. Enantiomer (4*R*,9*R*)-**14** was prepared using general procedure. Reaction of amine **10** (165 mg, 352 μmol) with active ester (4*R*,9*R*)-**2** (80 mg, 145 μmol) gave dimer (4*R*,9*R*)-**14** (91 mg, 51%) as a yellow powder.

Compound (4*R*,9*R*)-**14** has identical NMR spectra as **14**; $[\alpha]_D^{20}$ −182 (*c* 0.060 g/100 ml DMF).

4.11.2. Compound (4*S*,9*S*)-14. Enantiomer (4*S*,9*S*)-**14** was prepared using general procedure. Reaction of amine **10** (170 mg, 363 μmol) with active ester (4*S*,9*S*)-**2** (80 mg, 145 μmol) gave dimer (4*S*,9*S*)-**14** (128 mg, 72%) as a yellow powder.

Compound (4*S*,9*S*)-**14** has identical NMR spectra as **14**; $[\alpha]_D^{20}$ +183 (*c* 0.055 g/100 ml DMF).

Acknowledgements

Grant by the Ministry of Education of the Czech Republic MSM 6046137307, LC 512, grants 203/06/1038 and 305/05/2030 from Grant Agency of the Czech Republic, grant by the Ministry of Health of the Czech Republic NR 8355-3/2005, and EU grant 'CIDNA' NMP4-CT-2003-505669 supported the work.

Supplementary data

Supplementary data associated with this article can be found in the online version, at doi:10.1016/j.tet.2006.06.056.

References and notes

1. Johnson, D. S.; Boger, D. L. *Comprehensive Supramolecular Chemistry*; Murakami, Y., Atwood, J. L., Davies, J. E., MacNickol, D. D., Vögtle, F., Lehn, J.-M., Eds.; Pergamon: Oxford, 1996; pp 74–160.
2. Arcamone, F.; Nicolell, V.; Penco, S.; Orezzi, P.; Pirelli, A. *Nature* **1964**, *203*, 1064–1065.
3. Baraldi, P. G.; Tabrizi, M. A.; Preti, D.; Fruttarolo, F.; Avitabile, B.; Bovero, A.; Pavani, G.; Carretero, M. d. C. N.; Romagnoli, R. *Pure Appl. Chem.* **2003**, *75*, 187–194.
4. Dervan, P. B. *Bioorg. Med. Chem.* **2001**, *9*, 2215–2235.
5. Dervan, P. B.; Edelson, B. S. *Curr. Opin. Struct. Biol.* **2003**, *13*, 284–299.
6. Klevit, R. E.; Wemmer, D. E.; Reid, B. R. *Biochemistry* **1986**, *25*, 3296–3303.
7. Pelton, J. G.; Wemmer, D. E. *Biochemistry* **1988**, *27*, 8088–8096.
8. Coll, M.; Frederick, C. A.; Wang, A. H. J.; Rich, A. *Proc. Natl. Acad. Sci. U.S.A.* **1987**, *84*, 8385–8389.
9. Schultz, P. G.; Dervan, P. B. *Proc. Natl. Acad. Sci. U.S.A.* **1983**, *80*, 6834–6837.
10. Youngquist, R. S.; Dervan, P. B. *Proc. Natl. Acad. Sci. U.S.A.* **1985**, *82*, 2565–2569.
11. Kopka, M. L.; Yoon, C.; Goodsell, D.; Pjura, P.; Dickerson, R. E. *Proc. Natl. Acad. Sci. U.S.A.* **1985**, *82*, 1376–1380.
12. Lown, J. W.; Krowicki, K.; Bhat, G.; Skorobogaty, A.; Ward, B.; Dabrowiak, J. C. *Biochemistry* **1986**, *25*, 7408–7416.
13. Pelton, J. G.; Wemmer, D. E. *Proc. Natl. Acad. Sci. U.S.A.* **1989**, *86*, 5723–5727.
14. Pelton, J. G.; Wemmer, D. E. *J. Am. Chem. Soc.* **1990**, *112*, 1393–1399.
15. Mrksich, M.; Dervan, P. B. *J. Am. Chem. Soc.* **1993**, *115*, 2572–2576.
16. Wade, W. S.; Mrksich, M.; Dervan, P. B. *J. Am. Chem. Soc.* **1992**, *114*, 8783–8794.
17. Mrksich, M.; Parks, M. E.; Dervan, P. B. *J. Am. Chem. Soc.* **1994**, *116*, 7983–7988.
18. Swalley, S. E.; Baird, E. E.; Dervan, P. B. *J. Am. Chem. Soc.* **1996**, *118*, 8198–8206.
19. Szewczyk, J. W.; Baird, E. E.; Dervan, P. B. *Angew. Chem., Int. Ed.* **1996**, *35*, 1487–1489.
20. Bhattacharya, S.; Thomas, M. *Chem. Commun.* **2001**, 1464–1465.
21. Dyatkina, N. B.; Roberts, C. D.; Keicher, J. D.; Dai, Y.; Nadherny, J. P.; Zhang, W.; Schmitz, U.; Kongpachith, A.; Fung, K.; Novikov, A. A.; Lou, L.; Velligan, M.; Khorlin, A. A.; Chen, M. S. *J. Med. Chem.* **2002**, *45*, 805–817.
22. Fishleigh, R. V.; Fox, K. R.; Khalaf, A. I.; Pitt, A. R.; Scobie, M.; Suckling, C. J.; Urwin, J.; Waigh, R. D.; Young, S. C. *J. Med. Chem.* **2000**, *43*, 3257–3266.
23. Griffin, J. H.; Dervan, P. B. *J. Am. Chem. Soc.* **1986**, *108*, 5008–5009.

24. Khalaf, A. I.; Pitt, A. R.; Scobie, M.; Suckling, C. J.; Urwin, J.; Waigh, R. D.; Fishleigh, R. V.; Young, S. C.; Wylie, W. A. *Tetrahedron* **2000**, *56*, 5225–5239.
25. Khalaf, A. I.; Ebrahimabadi, A. H.; Drummond, A. J.; Anthony, N. G.; Mackay, S. P.; Suckling, C. J.; Waigh, R. D. *Org. Biomol. Chem.* **2004**, *2*, 3119–3127.
26. Kissinger, K. L.; Dabrowiak, J. C.; Lown, J. W. *Chem. Res. Toxicol.* **1990**, *3*, 162–168.
27. Lown, J. W.; Krowicki, K.; Balzarini, J.; Newman, R. A.; De Clercq, E. *J. Med. Chem.* **1989**, *32*, 2368–2375.
28. Rao, K. E.; Zimmermann, J.; Lown, W. J. *J. Org. Chem.* **1991**, *56*, 786–797.
29. Singh, M. P.; Plouvier, B.; Hill, C. G.; Gueck, J.; Pon, R. T.; Lown, W. J. *J. Am. Chem. Soc.* **1994**, *116*, 7006–7020.
30. Wang, W.; Lown, J. W. *J. Med. Chem.* **1992**, *35*, 2890–2897.
31. Bag, B. G. *Curr. Sci.* **1995**, *68*, 279–288.
32. Demeunynck, M.; Tatibouet, A. *Progress in Heterocycles Chemistry*; Gribble, G. W., Cilchrist, T. L., Eds.; Pergamon: Oxford, 1999; pp 1–20.
33. Valík, M.; Strongin, R. M.; Král, V. *Supramol. Chem.* **2005**, *17*, 347–367.
34. Bailly, C.; Laine, W.; Demeunynck, M.; Lhomme, J. *Biochem. Biophys. Res. Commun.* **2000**, *273*, 681–685.
35. Tatibouet, A.; Demeunynck, M.; Andraud, C.; Collet, A.; Lhomme, J. *Chem. Commun.* **1999**, 161–162.
36. Yashima, E.; Akashi, M.; Miyauchi, N. *Chem. Lett.* **1991**, 1017–1020.
37. Olsen, G. L.; Louie, E. A.; Drobny, G. P.; Sigurdsson, S. T. *Nucleic Acids Res.* **2003**, *31*, 5084–5089.
38. Tabernero, L.; Verdaguer, N.; Coll, M.; Fita, I.; Marel, G. A.; Boom, J. H.; Rich, A.; Aymamí, J. *Biochemistry* **1993**, *32*, 8403–8410.
39. Valík, M.; Dolenský, B.; Petříčková, H.; Vašek, P.; Král, V. *Tetrahedron Lett.* **2003**, *44*, 2083–2086.
40. Nishiwaki, E.; Tanaka, S.; Lee, H.; Shibuya, M. *Heterocycles* **1988**, *27*, 1945–1952.
41. Seltzman, H. H.; Berrang, B. D. *Tetrahedron Lett.* **1993**, *34*, 3083–3086.
42. Valík, M.; Dolenský, B.; Herdtweck, E.; Král, V. *Tetrahedron: Asymmetry* **2005**, *16*, 1969–1974.
43. Nishiwaki, E.; Nakagawa, H.; Takasaki, M.; Matsumoto, T.; Sakurai, H.; Shibuya, M. *Heterocycles* **1990**, *31*, 1763–1766.
44. Keiderling, T. A.; Silva, R. A. G. D.; Gorm, Y.; Dukor, R. K. *Bioorg. Med. Chem.* **1999**, *7*, 133–141.
45. Keiderling, T. A. *Circular Dichroism: Principles and Applications*; Berova, N., Nakanishi, K., Eds.; Wiley: New York, NY, 2000; pp 621–666.
46. Nafie, L. A.; Yu, G. S.; Freedman, T. B. *Vib. Spectrosc.* **1995**, *8*, 231–239.
47. Wang, L.; Keiderling, T. A. *Biochemistry* **1992**, *31*, 10265–10271.
48. Aamouche, A.; Devlin, F. J.; Stephens, P. J. *Chem. Commun.* **1999**, 361–362.
49. Palivec, L.; Urbanová, M.; Volka, K. *J. Pept. Sci.* **2005**, *11*, 536–545.
50. Urbanová, M.; Setnička, V.; Král, V.; Volka, K. *Biopolymers* **2001**, *60*, 307–316.
51. Nový, J.; Urbanová, M.; Volka, K. *J. Mol. Struct.* **2005**, *748*, 17–25.
52. Aamouche, A.; Devlin, F. J.; Stephens, P. J. *J. Am. Chem. Soc.* **2000**, *122*, 2346–2354.
53. Polavarapu, P. L. *J. Chem. Phys.* **1987**, *87*, 4419–4422.
54. Gunde, K. E.; Credi, A.; Jandrasics, E.; Zelewsky, A.; Richardson, F. S. *Inorg. Chem.* **1996**, *36*, 426–434.
55. Chen, F. M.; Sha, F. *Biochemistry* **1998**, *37*, 11143–11151.
56. Zhang, W.; Dai, Y.; Schmitz, U.; Bruice, T. W. *FEBS Lett.* **2001**, *509*, 85–89.
57. Johnson, W. *Circular Dichroism: Principles and Applications*; Berova, N., Nakanishi, K., Eds.; Wiley: New York, NY, 2000; pp 703–718.
58. Morgan, A. R.; Lee, J. S.; Pulleyblank, D. F.; Murray, N. L.; Evans, D. H. *Nucleic Acids Res.* **1979**, *7*, 547–569.
59. Wyatt, M. D.; Garbiras, B. J.; Haskell, M. K.; Lee, M.; Souhami, R. L.; Hartley, J. A. *Anti-Cancer Drug Des.* **1994**, *9*, 511–529.
60. Boger, D. L.; Fink, B. E.; Hedrick, M. P. *J. Am. Chem. Soc.* **2000**, *122*, 6382–6394.
61. Brabec, V.; Paleček, E. *Biophys. Chem.* **1976**, *4*, 76–92.
62. Urbanová, M.; Setnička, V.; Volka, K. *Chirality* **2000**, *12*, 199–203.